npg

ORIGINAL ARTICLE

Role of Lefty in the anti tumor activity of human adult liver stem cells

C Cavallari[1], V Fonsato[1], MB Herrera[1], S Bruno[2], C Tetta[2] and G Camussi[1]

Recent studies demonstrated that factors derived from embryonic stem cells inhibit the tumorigenicity of a variety of cancer cell lines. Embryonic stem cell-secreted Lefty, an inhibitor of Nodal-signalling pathway, was implicated in reprogramming cancer cells. Whether adult stem cells exhibited similar properties has not been explored. The aim of the present study was to investigate whether the conditioned medium (CM) derived from adult stem cells influence *in vitro* and *in vivo* tumor growth by a Nodal-dependent pathway. In particular we compared the anti-tumor effect of CM from human liver stem cells (HLSC) with that of bone marrow-derived mesenchymal stem cells (MSC). We found that HLSC-CM inhibited the *in vitro* growth and promoted apoptosis in HepG2 cells that expressed a deregulated Nodal pathway. The effect of HLSC-CM was related to the presence of Lefty A in the CM of HLSC. Silencing Lefty A in HLSC or Lefty A blockade with a blocking peptide abrogated the anti-proliferative and pro-apoptotic effect of HLSC-CM. Moreover, the administration of human recombinant Lefty A protein mimicked the effect of HLSC-CM indicating that Nodal pathway is critical for the growth of HepG2. At variance of HLSC, bone marrow-derived MSC did not express and release Lefty A and the MSC-CM did not exhibited an anti-tumor activity *in vitro*, but rather stimulated proliferation of HepG2. In addition, the intra-tumor administration of HLSC-CM was able to inhibit the *in vivo* growth of HepG2 hepatoma cells implanted subcutaneously in SCID mice. At variance, HLSC-CM derived from Lefty A silenced HLSC was unable to inhibit tumor growth. In conclusion, the results of present study suggest that Lefty A may account for the tumor suppressive activity of HLSC as a result of an inhibition of the Nodal-signalling pathway by a mechanism similar to that described for embryonic stem cells.

Oncogene (2013) **32,** 819–826; doi:10.1038/onc.2012.114; published online 2 April 2012

Keywords: lefty; tumor growth; adult stem cells; liver; hepatoma

INTRODUCTION

Recent studies demonstrated that the embryonic microenvironment inhibit the tumorigenicity of a variety of cancer cell lines.[1–5] Lee *et al.*[6] demonstrated that exposure of metastatic melanoma cells to an embryonic zebrafish microenvironment, before gastrulation, results in their reprogramming toward a nontumorigenic phenotype. In addition, when metastatic melanoma cells were transplanted into the chick embryonic microenvironment, the melanoma cells invaded host neural crest targets but did not form tumors, and a subset of these tumor cells were reprogrammed to a neural crest cell-like phenotype.[7,8] It is becoming increasingly clear that human embryonic microenvironment carried soluble factors that are able to block cancer cell proliferation by reducing their progression through the cell cycle, without affecting cell death.[9] Current studies showed that the human embryonic stem cell microenvironment specifically neutralizes the embryonic morphogen Nodal in metastatic melanoma and breast carcinoma cells, reprogramming them to a less aggressive phenotype.[2] Uncovered embryonic stem cell-secreted Lefty, an inhibitor of Nodal signalling, is one of the important mediator of these phenomena.[10–13] Nodal is an embryonic morphogen that belongs to TGF-beta super family involved in maintenance of embryonic stem cell pluripotency.[14,15] In several cancer cells the Nodal pathway is upregulated because of the absence of a regulatory mechanism.[16] In melanoma, Nodal pathway has been shown to sustain tumorigenicity and tumor cell plasticity and its inhibition may abrogate tumorigenesis. Similar results were found also in the growth of prostate cancer and in its progression.[17]

These studies demonstrated that the microenvironment of stem cells provides a previously unexplored therapeutic entity for the regulation of aberrantly expressed Nodal in aggressive tumor cells. Whether adult stem cells exhibited similar properties it is presently unknown. We recently identified a population of adult human liver stem cells (HLSC) that express a mesenchymal stem cell phenotype and several embryonic stem cell markers.[18]

The aim of the present study was to investigate whether the conditioned medium (CM) derived from HLSC (HLSC-CM) was able to influence tumor growth by a Nodal-dependent pathway. In particular we investigated whether HLSC expressed the key molecules of regulatory Nodal pathway such as Lefty and Cripto as the embryonic stem cells, and whether HLSC release Lefty in the medium. In addition, we investigate whether HLSC-CM was able to inhibit the growth of HepG2 hepatoma cells both *in vitro* and *in vivo* by a Lefty-dependent mechanism.

RESULTS

CM derived from HLSC decreases proliferation and induces apoptosis of HepG2 hepatoma cells

We investigated the effect of CM derived from six different HLSC lines on proliferation and apoptosis of HepG2 in comparison with CM obtained from six different human bone marrow-derived mesenchymal stem cells (MSC-CM). CM derived from all HLSC lines

820

significantly inhibited HepG2 proliferation in a dose-dependent manner. In contrast, all MSC-CM significantly stimulated HepG2 proliferation (Figures 1a and b). Moreover, HLSC-CM, but not MSC-CM, induced significant apoptosis of HepG2 (Figures 1c and d). The analysis of cell cycle demonstrated that HLSC-CM induced the appearance of a sub-G1 peak confirming cell apoptosis (Figure 1e). The subG1 peak was absent in HepG2 treated with MSC-CM. The anti-proliferative and pro-apoptotic effect of HLSC-CM was not liver specific as it was evident also on MCF7, KP6, KS, Jurkat cell lines, but not on SKOV3 and MAMM01 (Figures 1f and g).

Lefty A account for HLSC-CM induced decrease proliferation and apoptosis

HLSC, but not HepG2 and MSC, contained Lefty A as detected by western blot analysis, qRT–PCR and confocal microscopy

(Figures 2a–c). Lefty A was also detected in CM derived from HLSC (Figure 2a), suggesting an active release from these cells. The target protein of Lefty A, Nodal, an embryonal morphogen known to promote cell proliferation,[17] as well as Cripto, the co-receptor of Nodal, were expressed in HLSC, but not in MSC, suggesting an autocrine regulation of Lefty-Nodal pathway in HLSC similar to that described in embryonic stem cells.[2] On the other hand, HepG2 expressed Cripto and Nodal in the absence of Lefty expression, suggesting a deregulated pathway of Nodal-dependent proliferation (Figure 2c).

To investigate whether the anti-proliferative and pro-apoptotic effect of HLSC-CM was dependent on the presence of Lefty A we silenced Lefty A in HLSC by short hairpin RNA (shRNA). The reduction of Lefty A mRNA expression in HLSC was assessed by qRT–PCR (Figure 3a). The CM derived from HLSC (lane 1) and HLSC transfected with control vector (CTR scr; lane 2) expressed
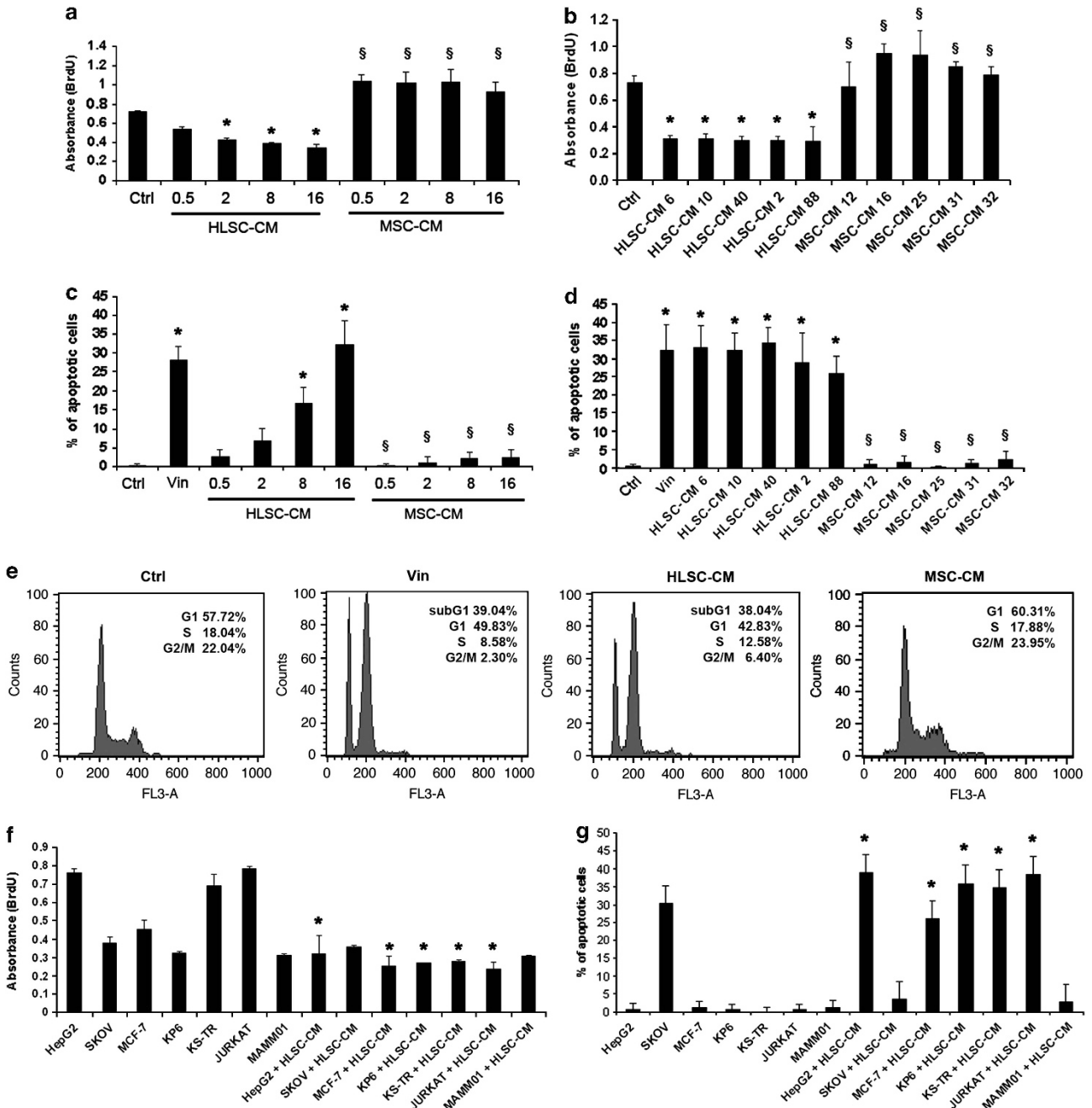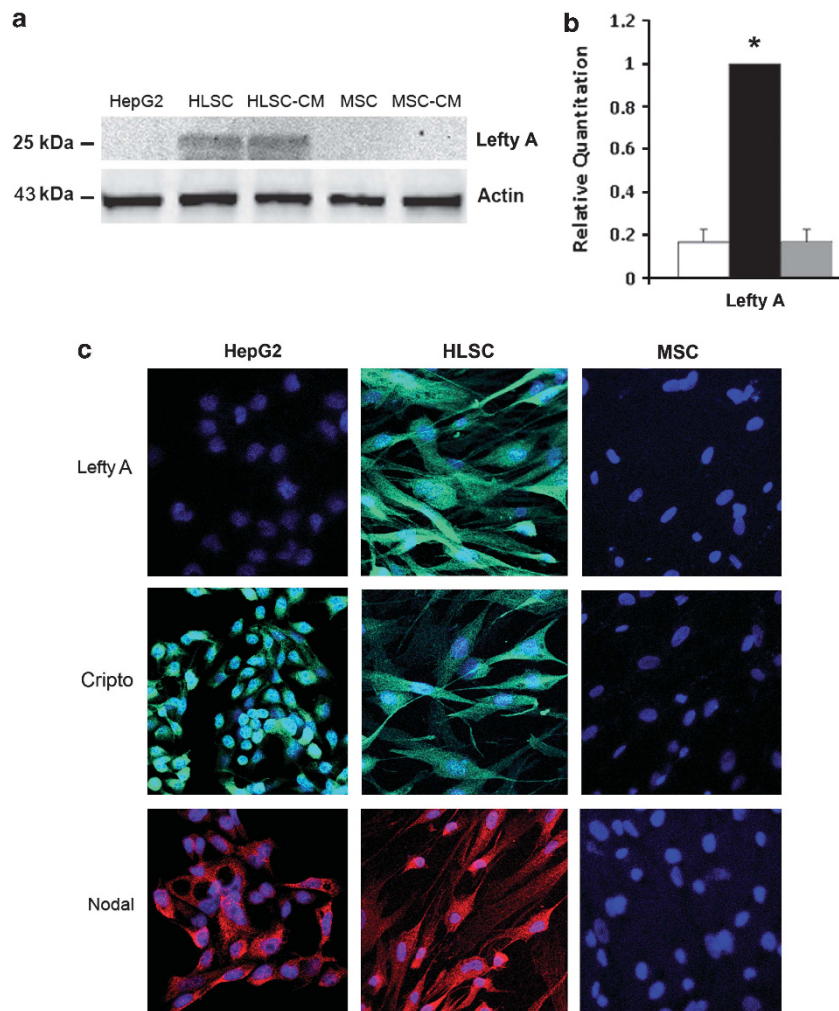
Figure 2. Expression and release of Lefty A by HLSC. (**a**) Representative western blot analysis showing Lefty A expression in HLSC, HLSC-CM, but not in HepG2, MSC and MSC-CM. Three experiments were performed with similar results. (**b**) qRT–PCR showing Lefty A mRNA expression in HLSC (black bar), but not in HepG2 (white bar), and in MSC (gray bar). Data are expressed as mean ± s.d. of three individual experiments. Analysis of variance (ANOVA) with Dunnet's multicomparison test was performed vs HepG2 (*$P<0.05$). (**c**) Representative confocal immunofluorescence micrographs showing the expression of Lefty A, Cripto and Nodal in HepG2, HLSC and MSC. Lefty A was expressed only in HLSC, whereas Cripto and Nodal were detected in HepG2 and HLSC but not in MSC. Control immunofluorescence after omission of the primary antibody or substitution with nonimmune rabbit IgG were negative. Four experiments were performed with similar results.

Figure 1. Proliferation and apoptosis of HepG2 induced by the CM of HLSC. (**a**) *In vitro* proliferation assay was performed incubating HepG2 cells with different dilutions of HLSC-CM or MSC-CM. Proliferation of HepG2 was evaluated by BrdU incorporation assay after 72 h of incubation. HepG2 were cultured in Dulbecco's modified Eagle's medium (DMEM) containing 10% FBS alone or supplemented with 0.5, 2, 8 or 16% of ×25-concentrated CM. Eight individual experiments were performed in quadruplicate. The data are expressed as mean ± s.d. analysis of variance (ANOVA) with Dunnet's multicomparison test was performed HLSC-CM vs Ctrl *$P<0.05$ and MSC-CM vs Ctrl *$P<0.05$. (**b**) *In vitro* proliferation assays performed on HepG2 cells incubated with 16% of ×25-concentrated HLSC-CM or MSC-CM obtained from six different cell preparations. The data are expressed as mean ± s.d. ANOVA with Dunnet's multicomparison test was performed HLSC-CM vs Ctrl *$P<0.05$ and MSC-CM vs Ctrl $^{\S}P<0.05$. (**c**) *In vitro* apoptosis assays was carried out by incubating HepG2 cells with different dilutions of HLSC-CM or MSC-CM. Apoptosis of HepG2 was evaluated by TUNEL assay as the percentage of apoptotic cells after 72 h of incubation with DMEM containing 10% FBS alone or supplemented with 0.5, 2, 8 or 16% of ×25-concentrated CM. Vincristine (10 ng/ml) was used as the positive control for apoptosis induction; in the negative control HepG2 were treated with vehicle alone. Five individual experiments were performed in quadruplicate. The data are expressed as mean ± s.d. ANOVA with Dunnet's multicomparison test was performed HLSC-CM vs Ctrl *$P<0.05$ and MSC-CM vs Ctrl not significant. (**d**) TUNEL assay performed on HepG2 incubated with 16% of ×25-concentrated HLSC-CM or MSC-CM obtained from six different cell preparations. Three individual experiments were performed in quadruplicate. The data are expressed as mean ± s.d. ANOVA with Dunnet's multicomparison test was performed HLSC-CM vs Ctrl *$P<0.05$ and MSC-CM vs Ctrl not significant. (**e**) Representative analysis of cell cycle of HepG2 treated with vehicle alone (Ctrl), Vincristine (10 ng/ml) as positive control, HLSC-CM (16%) or MSC-CM (16%) for 36 h. Results are representative of three independent experiments. (**f**) *In vitro* proliferation assays was performed incubating SKOV3, MCF7, KP6, KS-TR, Jurkat and MAMM01 cell lines with 16% of ×25-concentrated HLSC-CM. Proliferation of cells was evaluated by BrdU incorporation assay after 72 h of incubation. The data are expressed as mean ± s.d. ANOVA with Dunnet's multicomparison test was performed HLSC-CM vs HepG2, MCF7, KP6, KS-TR and Jurkat *$P<0.05$. (**g**) *In vitro* apoptosis assays was carried out by incubating SKOV3, MCF7, KP6, KS-TR, Jurkat and MAMM01 cell lines with 16% of ×25-concentrated HLSC-CM. Cell apoptosis was evaluated by TUNEL assay as the percentage of apoptotic cells after 72 h of incubation. Vincristine (10 ng/ml) was used as the positive control for apoptosis induction. Five individual experiments were performed in quadruplicate. The data are expressed as mean ± s.d. ANOVA with Dunnet's multicomparison test was performed HLSC-CM vs HepG2, MCF7, KP6, KS-TR and Jurkat *$P<0.05$.
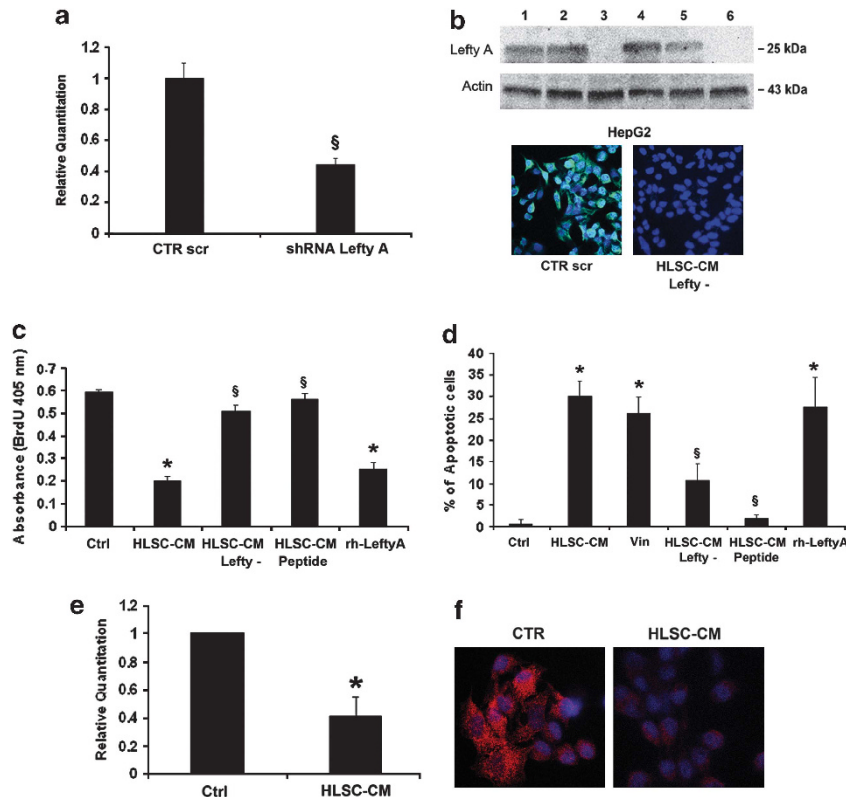
Figure 3. Silencing of Lefty A expression in HLSC abrogated the anti-proliferative and pro-apoptoic effects of HLSC-CM. (**a**) qRT−PCR showing the Lefty A mRNA downregulation in HLSC silenced with specific shRNA in respect to the high-level expression of mRNA in HLSC transfected with plasmid control vector. Data are expressed as mean ± s.d. of three individual experiments. (**b**) Representative western blot analysis showing Lefty A expression in CM derived from HLSC (lane 1) and HLSC transfected with control vector (CTR scr; lane 2) but not in Lefty A silenced HLSC (HLSC-CM Lefty⁻ lane 3). HepG2 stimulated with CM derived from HLSC (lane 4) or with CM derived from HLSC transfected with control vector (lane 5) expressed Lefty A, whereas when challenge with HLSC-CM Lefty⁻ did not. Representative immunofluorescence microscopy showing the *in vitro* downregulation of Lefty A protein in HepG2 when stimulated with Lefty A silenced HLSC compared with cells treated with CM derived from CTR scr. Three experiments were performed with similar results. (**c**) The effects on proliferation of HLSC-CM and silenced Lefty A HLSC were evaluated by BrdU incorporation after 72 h in the presence of vehicle alone (HepG2) or 16% of × 25 concentrated CM. Proliferation was not inhibited in HepG2 stimulated with HLSC-CM pre-incubated with the Lefty A blocking peptide, as in experiments with silenced Lefty A CM. In contrast pre-incubation of HLSC-CM with human recombinant protein Lefty A decreased proliferation in a manner comparable to that of HLSC-CM. Analysis of variance (ANOVA) with Newman−Keuls multicomparison test was performed: *$P < 0.05$ HLSC-CM and rh-Lefty A vs Ctrl; $§P < 0.05$ HLSC-CM Lefty⁻ and HLSC-CM peptide vs HLSC-CM. (**d**) Apoptosis was evaluated by Tunel assay. HepG2 were incubated with vehicle alone (HepG2) or with vincristine as apoptotic control. Apoptosis assay showed significant cell death in HepG2 stimulated with HLSC-CM comparable to that obtained with incubation of human recombinant protein Lefty A. Opposite effects were observed with silenced Lefty A HLSC and with HLSC-CM pre-incubated with the blocking peptide. ANOVA with Newman−Keuls multicomparison test was performed: *$P < 0.05$ HLSC-CM and rh-Lefty A vs Ctrl; $§P < 0.05$ HLSC-CM Lefty⁻ and HLSC-CM peptide vs HLSC-CM. (**e**) qRT−PCR showing the Nodal mRNA downregulation in HepG2 stimulated with HLSC-CM in respect to the high level expression of mRNA in control HepG2. Data are expressed as mean ± s.d. of three individual experiments. (**f**) Representative Immunofluorescence microscopy showing the *in vitro* downregulation of Nodal protein in HepG2 when stimulated with HLSC-CM compared with control HepG2. Three experiments were performed with similar results.

Lefty A, whereas Lefty A-silenced HLSC (HLSC-CM Lefty⁻ lane 3) did not, as seen by western blot analysis (Figure 3b). In addition, HepG2, that in basal condition did not express Lefty A (Figure 2a), when stimulated with CM derived from HLSC (lane 4) or with CM derived from HLSC transfected with control vector (lane 5) expressed Lefty A, whereas when challenge with HLSC-CM Lefty⁻ (lane 6) did not, as seen by western blot and confocal microscopy (Figure 3b). We therefore investigated the biological activity of CM derived from Lefty A-silenced cells. At variance of HLSC-CM, HLSC-CM Lefty⁻ did not inhibited proliferation or induced apoptosis of HepG2 (Figures 3c and d). In addition, the Lefty A blocking peptide abrogated the anti-proliferative and pro-apoptotic effect of HLSC-CM. These experiments suggested that Lefty blockade in HLSC-CM abrogated its biological effect on HepG2. Indeed the addition of human recombinant Lefty A (rh-Lefty A) significantly inhibited proliferation and stimulated apoptosis of HepG2 (Figures

3c and d). In addition, HLSC-CM inhibited Nodal expression both at mRNA and protein levels (Figures 3e and f).

HLSC-CM containing Lefty A inhibited HepG2 tumor growth *in vivo*
Subcutaneously injection of HepG2 in SCID mice generated tumors that became palpable after 1 week. At this time, mice were treated by intra-tumor injection of 20 μl of HLSC-CM or vehicle twice a week for 3 weeks. As shown in Figure 4, the tumor mass and weight were significantly reduced in mice injected with HLSC-CM, or rh-Lefty A in respect to those injected with vehicle (Figures 4a and b). In contrast, MSC-CM was found to enhance tumor mass. Histological analysis demonstrated an increased number of apoptotic cells as detected by Tunel, and a decreased number of PCNA-positive cells in tumors treated with HLSC-CM (Figure 4c). When CM obtained from Lefty silenced HLSC was
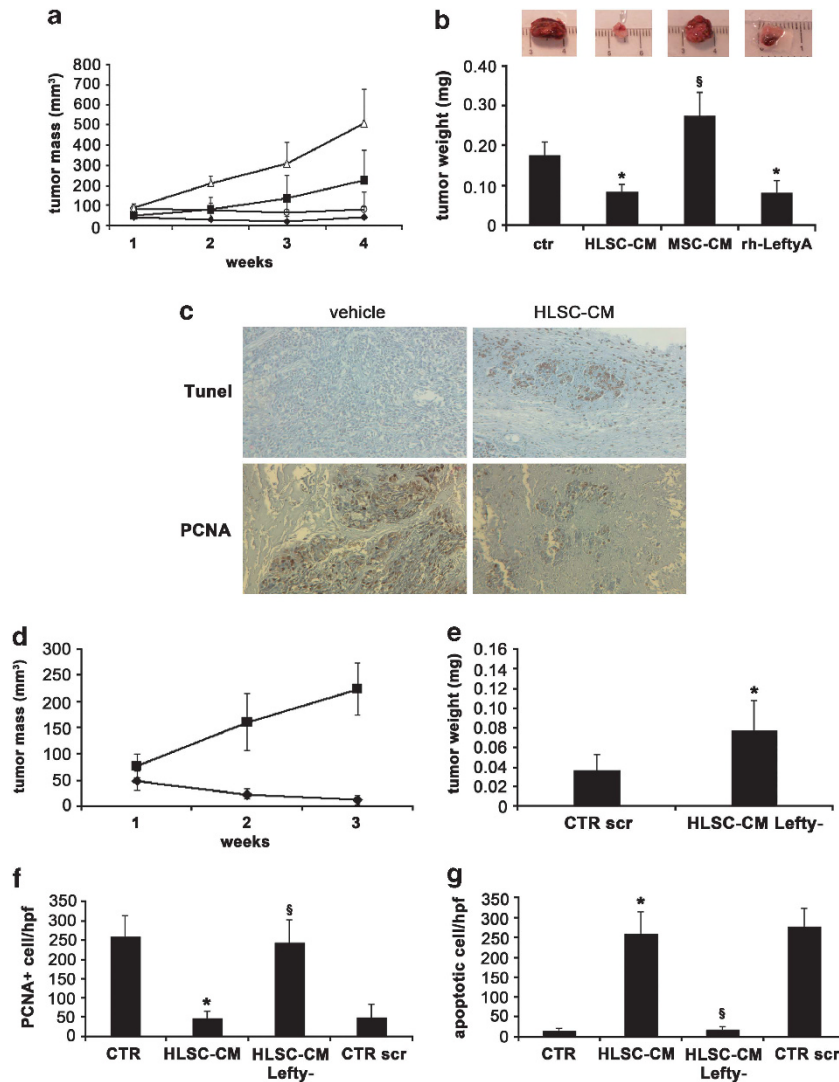
Figure 4. Effect of HLSC-CM, MSC-CM, rh-Lefty A and of HLSC-CM derived from Lefty A silenced HLSC on *in vivo* tumor growth, proliferation and apoptosis. (**a**) Tumor growth in SCID mice injected subcutaneously with 3×10^6 HepG2 and treated twice a week with 20 µl vehicle (■) or CM-HLSC (♦), or CM-MSC (▲) (100 µg proteins) or rh-Lefty A (○) protein (1 µg/ml). Tumor mass was determined twice a week by calliper measurement in two perpendicular diameters of the implant and calculated as described in Materials and methods. Each animal received two tumor implants and four animals per groups were studied. Data are expressed as mean ± s.d. (**b**) Tumor weights after excision from SCID mice at death. Data are expressed as mean ± s.d. Student's *t* test was performed: *$P < 0.05$ vehicle vs HLSC-CM and rh-Lefty A treatment; §$P < 0.05$ MSC-CM vs HLSC-CM and rh-Lefty A. (**c**) Representative micrographs of Tunel and PCNA immunohistochemical staining of tumors derived from SCID mice injected subcutaneously with HepG2 and treated twice a week with vehicle or HLSC-CM. Several apoptotic cells and only few PCNA-positive cells are visible in HepG2 tumors treated with HLSC-CM in respect to mice treated with vehicle. (**d**) Tumor growth in SCID mice injected subcutaneously with 3×10^6 HepG2 and treated twice a week with 100 µg of HLSC-CM scr (♦) or with HLSC-CM Lefty$^-$ (■). Each animal received two tumor implants and four animals per groups were studied. Data are expressed as mean ± s.d. Tumor mass was determined twice a week by calliper measurement in two perpendicular diameters of the implant and calculated as described in Materials and methods. (**e**) Tumor weight at death after HLSC-CM scr or with HLSC-CM Lefty$^-$ intra-tumor treatment. Data are expressed as mean ± s.d. Student's *t* test was performed: *$P < 0.05$ HLSC-CM Lefty$^-$ vs HLSC-CM scr treatment. (**f**) Quantification of PCNA-positive cells/high power field (hpf). Data are expressed as mean ± s.d. of four mice for experimental group. analysis of variance (ANOVA) with Newmann–Keuls multi-comparison test was performed: *$P < 0.05$ HLSC-CM vs vehicle alone (CTR); §$P < 0.05$ HLSC-CM Lefty$^-$ vs HLSC-CM scr. (**g**) Quantification of TUNEL-positive cells/high power field (hpf). Data are expressed as mean ± s.d. of four mice for experimental group. ANOVA with Newmann–Keuls multicomparison test was performed: *$P < 0.05$ HLSC-CM vs vehicle alone (CTR); §$P < 0.05$ HLSC-CM Lefty$^-$ vs HLSC-CM scr.

used, the anti-tumor effect of HLSC-CM was significantly reduced (Figures 4d–g).

DISCUSSION

The results of the present study demonstrated that the CM derived from HLSC inhibits the growth of HepG2 and promotes their apoptosis both *in vitro* and *in vivo*. These biological effects

were related to the release within CM of Lefty A from HLSC. Indeed, silencing Lefty A or Lefty A blockade abrogated the anti-proliferative and pro-apoptotic effect of HLSC-CM. At variance of HLSC, bone marrow-derived MSC did not express and release Lefty A and the MSC-CM stimulated *in vitro* proliferation of HepG2.

Previous studies on embryonic stem cell microenvironment demonstrated that the release of Lefty may inhibit the Nodal

pathway in metastatic cancer cells and abrogate their tumorigenicity.[2] In normal adult cells the integral component of this pathway such as Cripto, the Nodal co-receptor, as well as Nodal and its negative regulator Lefty A are not expressed. At variance, the Nodal pathway was shown to be constitutively activated in many cancer cells as it occurs in embryonic cells. However, at variance of embryonic stem cells, the negative regulator Lefty A is absent in cancer cells.[2,17]

In embryonic stem cells, DNA methylation is thought to be one of the factors that regulate the expression of Lefty A. Indeed high-level expression of Lefty A by embryonic stem cells was shown to depend on the presence of an unmethylated form of the gene. The methylated status of Lefty A in melanoma cells could explain their incompetence to produce this inhibitor.[19] Moreover, it has been shown that Lefty A is post-transcriptionally targeted by miR-302 resulting in a negative modulation of its expression. This microRNA-dependent regulation of Lefty synthesis in embryonic stem cells may be critical for the equilibrium between pluripotency and germ layer specification.[20]

The HepG2 hepatoma cells used in the present study constitutively express Nodal and its co-receptor Cripto, but did not express Lefty A suggesting a deregulated Nodal pathway in these cancer cells. On the other hand, we found that HLSC expressed as the embryonic stem cells, the different component of Nodal pathway, including Lefty A. This make HLSC different from bone marrow-derived MSC that did not express any of the component of Nodal pathway. In addition, HLSC are known to be positive for several embryonic factors, including nanog, Oct-4, Sox2 and SSEA-4.[21] However, at variance of embryonic stem cells, HLSC are not pluripotent and do not form teratoma, but they are only multipotent as they differentiate in hepatocytes, osteocytes, adipocytes, endothelial and islet-like cells under specific culture conditions.[18]

In the present study, we found that the CM of HLSC inhibited proliferation and enhanced apoptosis of HepG2 *in vitro* and induced HepG2 tumor regression *in vivo*. The dependency of these biological effects on the presence of Lefty in HLSC-CM was shown from experiments of Lefty downregulation in HLSC and on the use of a Lefty blocking peptide that significantly inhibited the anti-proliferative and pro-apoptotic effects of HLSC-CM. Lefty downregulation also prevented the inhibitory effect of HLSC-CM on HepG2 tumor growth in SCID mice. Moreover, the administration of human recombinant Lefty A protein mimicked the effect of HLSC-CM indicating that Nodal pathway is critical for growth of HepG2 tumors. When the CM derived from MSC that do not contain Lefty A was used, no inhibitory effect on proliferation or induction of apoptosis was observed. All together these results suggest that the anti-tumor effect of HLSC-CM depends on the release of Lefty from HLSC.

In conclusion, results of the present study indicate that Lefty A may account for the tumor suppressive activity of HLSC as result of an inhibition of the Nodal-signalling pathway.

Despite the potential anti-tumor activity of embryonic stem cells, their clinical use is limited by an allogeneic immune response in the recipient and they may pose ethical problems. The present study suggest that HLSC display anti-tumor activity with a mechanism similar to that of embryonic stem cells and provide a possible alternative cell source for the treatment of tumors.

MATERIALS AND METHODS

Isolation and characterization of adult HLSC, HepG2 and MSC

HLSC were isolated from human cryopreserved normal hepatocytes obtained from Cambrex Bio Science Verviers S.p.r.l. (Cambrex Bio Science, Verviers, Belgium) cultured in minimum essential medium/endothelial cell basal medium-1 (α-MEM/EBM) (3:1) (Cambrex Bio Science) supplemented with ʟ-glutamine (5 mᴍ), Hepes (12 mᴍ, pH 7.4), penicillin (50 IU/ml), streptomycin (50 μg/ml) (all from Sigma-Aldrich, St Louis, MO, USA), fetal

bovine serum (FBS, 10%) as previously described.[18,21] The expanded cells were transferred to a T-75 flask and analyzed when they approached confluence.

MSC were obtained from Lonza (Basel, Switzerland), cultured and characterized as previously described.[22] The mononucleated cells were cultured in the presence of MSC basal medium (Lonza).

HLSC and MSC were used within the sixth passage of culture. At each passage, cells were counted and analyzed by cytofluorimetric analysis and immunofluorescence to confirm their phenotype. Cells were characterized by FACS analysis for the expression of mesenchymal stem cell markers, and in the case of HLSC also for the expression of tissue-specific markers, including α-fetoprotein and human albumin and of resident stem cell markers, such as vimentin and nestin, as previously described.[18,21] Moreover, HLSC were negative for the oval cell markers CD34, CD117 and cytokeratin 19 and express the embryonic stem cell markers nanog, Oct4, SOX2 and SSEA-4.[18,21] Both the cell types were able to undergo osteogenic, adipogenic and chondrogenic differentiation when cultured in the appropriate differentiative media.[18,22] HLSC were also able to differentiate in mature hepatocytes.

Hepatoma cell line HepG2 (American Type Culture Collection, Rockville, MD, USA) were cultured in Dulbecco's modified Eagle's medium containing 10% FBS. MCF7 (breast cancer cell line), Jurkat T cells (acute T-cell leukemia), KP-6 (prostate carcinoma cell line) and KS (Kaposi's sarcoma cells) were cultured in RPMI 1640 (Invitrogen, Carlsband, CA, USA) supplemented with 10% FBS.[23] MAMM01 (mammary carcinoma cell line) were cultured in EBM supplemeted with 10% FBS. SKOV3 (ovarian cancer cell line) were cultured in IMDM supplemented with 10% FBS.

Western blot analysis

Thirty micrograms of total cell lysate from HepG2, HLSC, MSC or conditioned media derived from HLSC, HLSC transfected with shRNA control vector, HLSC transfected with Lefty A-shRNA and HepG2 treated for 72 h with these conditioned media were loaded onto a 4–15% Mini-PROTEAN TGX (Bio-Rad, Hercules, CA, USA), and next electroblotted onto nitrocellulose membrane filters. Cells were lysed at 4 °C for 1 h in a lysis buffer (50 mmol/l Tris-HCl, pH 8.3, 1% Triton X-100, 10 mol/l phenylmethyl sulfonyl fluoride, 10 mol/l leupeptin, and 100 U/ml aprotinin) and centrifuged at 15 000 g. The protein contents of the supernatants were measured by the Bradford method. The blots were blocked with 5% nonfat milk in 20 mmol/l Tris-HCl, pH 7.5, 500 mmol/l NaCl plus 0.1% Tween (TBS-T). The membranes were subsequently immunoblotted overnight at 4 °C with Lefty antibody (antibody sc-7408, Santa Cruz Biotechnology, Santa Cruz, CA, USA), at the appropriate concentration. The membranes were then stripped and reprobed for actin (antibody sc-8432, Santa Cruz Biotechnology) as a protein loading control.

After extensive washings with TBS-T, the blots were incubated for 1 h at room temperature with peroxidase-conjugated isotype-specific secondary antibodies (Santa Cruz Biotechnology), washed with TBS-T, developed with ECL detection reagents (Amersham, Buckinghamshire, UK) for 1 min, and analyzed by Chemidoc XRS Bio-Rad.

Immunofluorescence

Indirect immunofluorescence was performed on HepG2, HLSC and MSC fixed in 4% paraformaldehyde containing 2% sucrose and when needed, permeabilized with Hepes-Triton X 100 buffer. The following polyclonal antibodies were used: anti-Lefty (antibody sc-7408), anti-Cripto (antibody sc-23369) and anti-Nodal (antibody sc-28913) antibodies all from Santa Cruz Biotechnology. Omission of the primary antibody or substitution with nonimmune rabbit IgG was used as controls. Alexa Fluor 488 anti-goat IgG and Alexa Fluor 594 anti-rabbit IgG were used as secondary Ab. Confocal microscopy analysis was performed using a Zeiss LSM 5 Pascal Model Confocal Microscope (Carl Zeiss International, Oberkochen, Germany). Hoechst 33258 dye (Sigma-Aldrich) was added for nuclear staining.

Silencing of Lefty A expression in HLSC

The knock down of Lefty A was obtained by transfection of HLSC with a specific Lefty A shRNA plasmid (NM_003240.2-990s1c1, Sigma-Aldrich)

using lipofectamine technique (lipofectamine 2000, Invitrogen). Transfection with a control plasmid coding for a scramble shRNA sequence (MISSION Nontarget shRNA Control Vector, SHC002, Sigma-Aldrich) was used as control. Cells were grown in the presence of 100 ng/ml puromycin according to the manufacturer's protocol to select stably transfected HLSC. Cells from transfected control (CTR scr) and knockdown Lefty A HLSC were harvested and tested for the specific Lefty A expression.

RNA extraction and quantitative real time–PCR

Total RNA was isolated from HepG2, MSC and HLSC using the mirVana RNA isolation kit (Ambion Inc., Austin, TX, USA) according to the manufacturer's protocol. RNA was then quantified by spectrophotometer (Nanodrop ND-1000, Nanodrop, Wilmington, DE, USA).

First strand DNA was produced from 1 µg of total RNA using High cDNA Reverse Transcription Kit (Applied Biosystems, Foster City, CA, USA). Briefly, 1 µg of mRNA, 2 µl of RT buffer, 0.8 µl of dNTP mixture, 2 µl of RT random primers, 1 µl of Multi-Scribe reverse transcriptase and 4.2 µl of nuclease-free water were used for each cDNA synthesis. After the reverse transcription, cDNA was stored at −20 °C.

Quantitative Real time PCR (qRT–PCR) was performed using the Power SYBR Green PCR Master Mix purchased from Applied Biosystems on a 96-well StepOnePlus Real Time System (Applied Biosystems). qRT–PCR to evaluate mRNA expression in CTR scr and shRNA Lefty A HLSC was performed using the following sequence-specific oligonucleotide primers (purchased from MWG-Biotech AG, Ebersberg, Germany): hLEFTYA: forward, 5′-GAG GTG CCC GTA CTG GAC AG-3′ and reverse 5′-GCC ACC TCT CGG AAG CTC-3′, hGAPDH: forward, 5′-TGG AAG GAC TCA TGA CCA CAG T-3′ and reverse 5′-CAT CAC GCC ACA GTT TCC C-3′. Nodal forward, 5′-GGC GAG TGT CCT AAT CCT GTT G-3′ and reverse 5′-CGT TTC AGC AGA CTC TGG ATG T-3′.

Primers were designed with Primer Express software (Applied Biosystems). The threshold cycle (Ct), the cycle number at which the amount of amplified gene of interest reached a fixed threshold, was subsequently determined. Real-time PCR experiments were performed in 20 µl reaction mixture containing 2.5 ng of cDNA template. Thermal-cycling conditions were as follows: activation of AmpliTaq Gold DNA Polymerase LD at 95 °C for 10 min, followed by 40 cycles of amplification at 95 °C for 15 s and 60 °C for 1 min. For all real-time PCR analyses, GAPDH mRNA was used to normalize RNA inputs.

Concentration of CM from HLSC

Supernatants of MSC, HLSC, CTR scr and shRNA Lefty A HLSC (HLSC-CM Lefty), cultured in MEM-alpha supplemented with 2% of FBS were collected after 24 h. Supernatants of MSC were obtained culturing MSC in RPMI deprived of FBS and supplemented with 0.5% of BSA (Sigma-Aldrich). The viability of cells was detected by trypan blue exclusion. After centrifugation at 3000 g for 10 min to remove cell debris, cell-free supernatants were ultracentrifuged at 40 000 g (Beckman Coulter Optima L-90K) for 1 h at 4 °C to remove microvesicles and membranes. The experiments were performed with a cell free CM harvested from a cell mass of 1.5×10^6 cells. The medium was then concentrated ~25 fold by centrifugation at 2700 g for 75 min, using Ultra-PL 3 ultrafiltration units (Amicon-Millipore Concord Road, Billerica, MA, USA) with a 3-kDa molecular weight cutoff. A total of 250 µl of CM was obtained.

Cell proliferation assay

All cancer cell lines (8×10^3/well) were cultured in Dulbecco's modified Eagle's medium containing 10% FBS in 96-well plate in the presence or absence of CM derived from HLSC, MSC or silenced HLSC. In selected experiments recombinant human Lefty A (1 µg/ml) (746-LF/CF, R&D Systems, Minneapolis, MN, USA) and blocking peptide (25 ng/ml) (sc-7408P, Santa Cruz) were used for control experiments.

DNA synthesis was detected as incorporation of 5-bromo-2-deoxyuridine (BrdU) into the cellular DNA using an enzyme-linked immunosorbent assay kit (Chemicon, Temecula, CA, USA) according to the manufacturer's instructions. Briefly, after washing, cells were incubated with 10 mol/l BrdU

for 12 h at 37 °C, 5% CO2, in a humidified atmosphere, fixed with 0.5 mol/l ethanol/HCl and incubated with nuclease to digest DNA. BrdU incorporated into the DNA was detected using an anti-BrdU peroxidase-conjugated monoclonal antibody and visualized with a soluble chromogenic substrate. Optical density was measured with an enzyme-linked immunosorbent assay reader at 405 nm.

Apoptosis assay

Apoptosis was evaluated using the terminal dUTP nickend-labeling assay (ApoTag; Oncor, Gaithersburg, MD, USA). Cells (8×10^3/well) were cultured in 96-well plate, suspended in phosphate-buffered saline (PBS) and fixed in 1% paraformaldehyde in PBS, pH 7.4, for 15 min at 4 °C followed by fixation with precooled ethanol/acetic acid (2:1) for 5 min at −20 °C. Cells were treated with terminal deoxynucleotide transferase enzyme and incubated in a humidified chamber for 1 h at 37 °C and then treated with fluorescein isothiocyanate-conjugated antidigoxigenin for 30 min at room temperature. After washing, samples were mounted in medium containing 1 µg/ml of propidium iodide and the cells were analyzed by immunofluorescence.

DNA cell cycle analysis

Cells were plated at a density of 100 000 cells in 5 ml of growth medium in T25 flasks with different treatment conditions for 36 h. Cells were fixed in 70% cold ethanol overnight at −20 °C, washed in PBS, Triton 0.5% and resuspended in PBS solution with 0.1% Triton containing 100 µg/ml of propidium iodide and 100 µg/ml of RNase type A for 4 h at +4 °C. Flow citometry analysis was performed after gating to eliminate doublets and debris.

Model of regression of an established tumor

Animal studies were approved and conducted in accordance with the National Institute of Health Guide for the Care and Use of Laboratory Animals and the institutional review board approved the protocol. Male 4- to 5-weeks-old SCID mice were obtained from Charles River laboratories, Inc., Wilmington, MA, USA. All mice were housed in a clean facility and held for 1 week to acclimatize. On day 0, each mouse received in the left and right flank subcutaneous injections (3×10^6 each) of HepG2 tumor cells resuspended in serum-free Dulbecco's modified Eagle's medium with Matrigel basement membrane matrix at a 1:1 ratio. Cell suspension was injected in a total volume of 0.2 ml. Tumors became palpable after 7 days and reached a volume of ~15 mm³. At this time mice were randomized into the four treatment groups and injected twice a week within the tumor with 100 µg in 20 µl of: HLSC-CM ($n = 4$), vehicle (cell culture medium submitted to the same concentration protocol of CM; $n = 4$), MSC-CM ($n = 4$), rh-Lefty A ($n = 4$), CTR scr HLSC-CM ($n = 4$) or HLSC-CM Lefty⁻ ($n = 4$). The animals were monitored for activity and physical condition everyday, and the determination of body weight and measurement of tumor mass were done every 3 days. Tumor mass was determined by calliper measurement in two perpendicular diameters of the implant and calculated using the formula $1/2a \times b^2$, where a stands for the long diameter and b is the short diameter. Animals were killed on day 21 and tumors were excised, weighted and submitted to histological analysis.

Morphological studies

Tumors were fixed in 10% buffered neutral formalin, routinely processed, embedded in paraffin, sectioned at 5 µm and stained with H and E for microscopic examination. Immunohistochemistry for detection of proliferation and apoptosis was performed using the anti-PCNA monoclonal antibody (Santa Cruz Biotechnology) or TUNEL, respectively, as previously described.[21]

Statistical analysis

All data of different experiments were expressed as average ± s.d. Statistical analysis was performed by analysis of variance with Dunnet's or Newmann–Keuls multi-comparison tests or by Student's t-tests (unpaired, two-tailed) where appropriated.

826

REFERENCES

1 Díez-Torre A, Andrade R, Eguizábal C, López E, Arluzea J, Sili M *et al.* Reprogramming of melanoma cells by embryonic microenvironments. *Int J Dev Biol* 2009; **53**: 1563–1568.

2 Postovit LM, Margaryan V, Seftor EA, Kirschmann DA, Lipavsky A, Wheaton WW *et al.* Human embryonic stem cell microenvironment suppresses the tumorigenic phenotype of aggressive cancer cells. *Proc Natl Acad Sci USA* 2008; **105**: 4329–4334.

3 Hendrix MJ, Seftor EA, Kasemeier-Kulesa J, Kulesa PM, Postovit LM. Reprogramming metastatic tumour cells with embryonic microenvironments. *Nat Rev Cancer* 2007; **7**: 246–255.

4 Postovit LM, Seftor EA, Seftor EB, Hendrix MJ. A three-dimensional model to study the epigenetics effects induced by the microenvironment of human embryonic stem cells. *Stem cells* 2005; **24**: 501–505.

5 Pierce GB, Pantazis CG, Caldwell JE, Wells RS. Specificity of the control of tumor formation by the blastocyst. *Cancer Res* 1982; **42**: 1082–1087.

6 Lee LM, Seftor EA, Borde G, Cornell RA, Hendrix MJ. The fate of human malignant melanoma cells transplanted into zebrafish embryos: assessment of migration and cell division in the absence of tumor formation. *Dev Dyn* 2005; **233**: 1560–1570.

7 Kulesa P, Kasemeier-Kulesa JC, Teddy JM, Margaryan NV, Seftor EA, Seftor RE *et al.* Reprogramming metastatic melanoma cells to assume a neural crest cell-like phenotype in an embryonic microenvironment. *Proc Natl Acad Sci USA* 2006; **103**: 3752–3757.

8 Podesta AH, Mullins J, Pierce GB, Wells RS. The neurula stage mouse embryo in control of neuroblastoma. *Proc Natl Acad Sci USA* 1984; **81**: 7608–7611.

9 Giuffrida D, Rogers IM, Nagy A, Calogero AE, Brown TJ, Casper RF. Human embryonic stem cells secrete soluble factors that inhibit cancer cell growth. *Cell Prolif* 2009; **42**: 788–798.

10 Sakuma R, Ohnishi Yi Y, Meno C, Fujii H, Juan H, Takeuchi J *et al.* Inhibition of Nodal signalling by Lefty mediated through interaction with common receptors and efficient diffusion. *Genes Cells* 2002; **7**: 401–412.

11 Meno C, Takeuchi J, Sakuma R, Koshiba-Takeuchi K, Ohishi S, Saijoh Y *et al.* Diffusion of nodal signaling activity in the absence of the feedback inhibitor Lefty2. *Dev Cell* 2001; **1**: 127–138.

12 Meno C, Gritsman K, Ohishi S, Ohfuji Y, Heckscher E, Mochida K *et al.* Mouse Lefty2 and zebrafish antivin are feedback inhibitors of nodal signaling during vertebrate gastrulation. *Mol Cell* 1999; **4**: 287–298.

13 Dvash T, Sharon N, Yanuka O, Benvenisty N. Molecular analysis of LEFTY-expressing cells in early human embryoid bodies. *Stem Cells* 2007; **25**: 465–472.

14 Abbott DE, Bailey CM, Postovit LM, Seftor EA, Margaryan N, Seftor RE *et al.* The epigenetic influence of tumor and embryonic microenvironments: how different are they? *Cancer Microenviron* 2008; **1**: 13–21.

15 Tabibzadeh S, Hemmati-Brivanlou A. Lefty at the crossroad of 'stemness' and differentiative events. *Stem Cells* 2006; **24**: 1998–2006.

16 Topczewska JM, Postovit LM, Margaryan NV, Sam A, Hess AR, Wheaton WW *et al.* Embryonic and tumorigenic pathways converge via Nodal signaling: role in melanoma aggressiveness. *Nat Med* 2006; **12**: 925–932.

17 Lawrence MG, Margaryan NV, Loessner D, Collins A, Kerr KM, Turner M *et al.* Reactivation of embryonic nodal signalling is associated with tumor progression and promotes the growth of prostate cancer cells. *The Prostate* 2011; **71**: 1198–1209.

18 Herrera MB, Bruno S, Buttiglieri S, Tetta C, Gatti S, Deregibus MC *et al.* Isolation and characterization of a stem cell population from adult human liver. *Stem Cells* 2006; **24**: 2840–2850.

19 Costa FF, Seftor A, Bischof JM, Kirschmann DA, Strizzi L, Arndt K *et al.* Epigenetically reprogramming metastatic tumor cells with an embryonic microenvironment. *Epigenomics* 2009; **1**: 387–398.

20 Barroso-delJesus A, Lucena-Aguilar G, Sanchez L, Ligero G, Gutierrez-Aranda I, Menendez P. The Nodal inhibitor Lefty is negatively modulated by the microRNA miR-302 in human embryonic stem cells. *FASEB J* 2011; **25**: 1479–1508.

21 Herrera MB, Fonsato V, Gatti S, Deregibus MC, Sordi A, Cantarella D *et al.* Human liver stem cell-derived microvesicles accelerate hepatic regeneration in hepatectomized rats. *J Cell Mol Med* 2010; **14**: 1605–1618.

22 Bruno S, Grange C, Deregibus MC, Calogero RA, Saviozzi S, Collino F *et al.* Mesenchymal stem cell-derived microvescicles protect against acute tubular injury. *J Am Soc Nephrol* 2008; **20**: 1053–1067.

23 Deregibus MC, Cantaluppi V, Doublier S, Brizzi MF, Deambrosis I, Albini A *et al.* HIV-1-Tat protein activates phosphatidylinositol 3-kinase/AKT-dependent survival pathways in Kaposi's sarcoma cells. *J Biol Chem* 2002; **28**: 25195–25202.